

Supporting information

Polarization Properties of Semiconductor Nanorod Heterostructures: From Single Particles to the Ensemble

*Ido Hadar, Gal B. Hitin, Amit Sitt, Adam Faust, Uri Banin**

Institute of Chemistry and the Center for Nanoscience and Nanotechnology, The Hebrew
University, Jerusalem 91904, Israel

Corresponding author e-mail address – banin@chem.ch.huji.ac.il.

1. Improved signal to noise ratio by simultaneous measurement of two polarization components

In some of the measurements we observed blinking in the emission of the nanorods, which causes large fluctuations in the emission intensity between subsequent frames (or wave-plate angles). Due to these changes in emission intensity, interpretation of the raw data is difficult and sometimes impossible as can be seen in figure S1a. Figure S1b shows how simple calculation of the polarization factor, for each frame (and wave-plate angle) independently allows us to overcome these strong fluctuations in intensity, and obtain the sinusoidal behavior, which describes linearly polarized emission. This feature arises from the simple fact that the polarization is not dependent at the overall intensity but only on the ratio between the two polarization components, which is not changing during blinking.

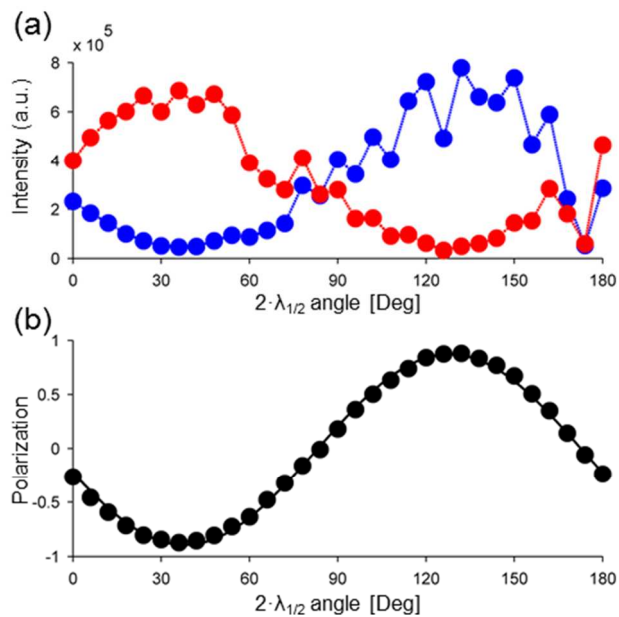


Figure S1. Representative measurement of single nanorod showing blinking. (a) Raw intensity of the horizontal (blue) and vertical (red) polarization components at different half wave-plate angles (lines are guide for the eye). (b) Polarization factor calculated from the raw intensity (Black dots) and sinusoidal fit to the polarization factor (Black line), both showing improved S/N in comparison to the raw data.

2. Correlation between Optical image and AFM scan

In order to correlate the optical image and the AFM scan the location of the AFM tip with respect to the optical image need to be found. First, a conversion matrix between the AFM coordinates (given as displacement from the tip native location in length units) and the optical image coordinates (given as pixels in the optical image) is acquired. This procedure is done by taking 25 optical images of the AFM cantilever at known displacements (Figure S2a). The contour of the cantilever is found for each image, and the conversion matrix is constructed by calculating the shift in the optical image. This procedure is done automatically by the AFM software (JPK DirectOverlay). Next, the exact location of the AFM tip relative to the cantilever is obtained by imaging the scattering from the tip apex. This is done by comparing two images taken on the same frame, with and without the tip, while illuminating the sample from below with white light. In the image with the tip a brighter spot can be seen, corresponding to scattering from the apex of the tip (see figure S2b). Afterwards, an optical image which has the AFM coordinates is obtained, and by shifting the AFM tip we can scan the same nanorods previously seen in the optical image, as can be seen in figure S2c.

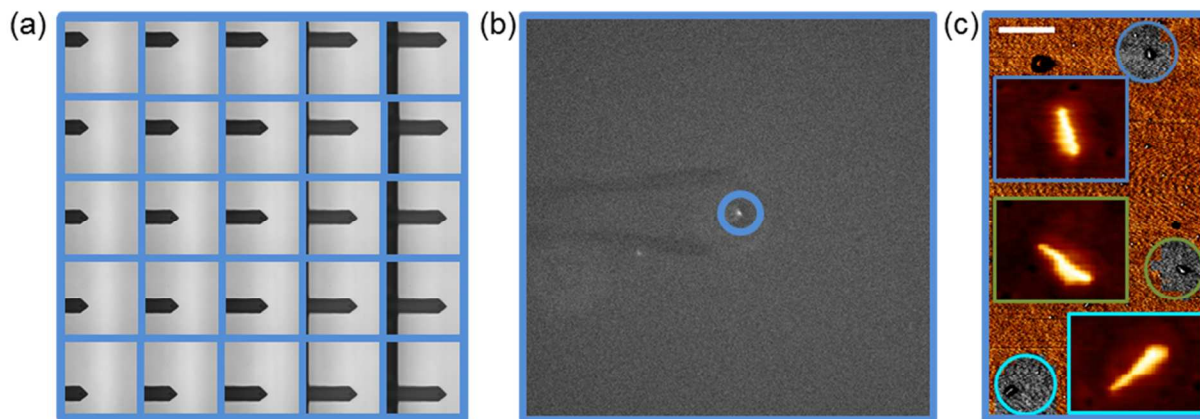


Figure S2. Correlated AFM and optical image. (a) Optical image of the AFM cantilever at known locations. (b) White light scattering image of the sample, with the tip. Blue circle represents the assumed tip apex manifested by scattering feature. (c) AFM scan overlaid by correlated optical image of emission from single nanorods (gray spots mark diffraction limited spots in the optical image), insets show detailed scan of the nanorods (scale bar is 500nm for the overall image & 70nm for the zoomed-in AFM scan insets).

3. Sample with broad size distribution

The strength of the single particle method in comparison to ensemble methods can be seen when examining systems with relatively large size distribution. In order to demonstrate this we present here analysis for a nanorod sample with average dimensions of 49 nm x 5 nm which shows relatively wide size distribution in comparison to the samples shown in the main text. This broadening can be seen in TEM images (see figure S3a) and also as a broadening of the sharp transitions in the absorption spectrum and broader emission spectrum (see figure S3b). Single particle polarization measurements show that for these samples a wider distribution of the polarization factor is obtained as well. This is due to larger variance in the single nanorods physical structure, causing modifications in the electronic structure and thus in the degree of polarization. Figure S3c shows a histogram of the polarization factor for the sample with wider size distribution showing average degree of polarization of 0.74 with standard deviation of 0.09. Although the average polarization obtained is almost the same as for the S@R sample with the narrow size distribution ($p=0.75$), the width of the histogram is significantly different. In ensemble polarization anisotropy measurements in solution, both samples show nearly identical anisotropy data and only single particle measurement reveals the fundamental differences arising from the underlying particle distribution.

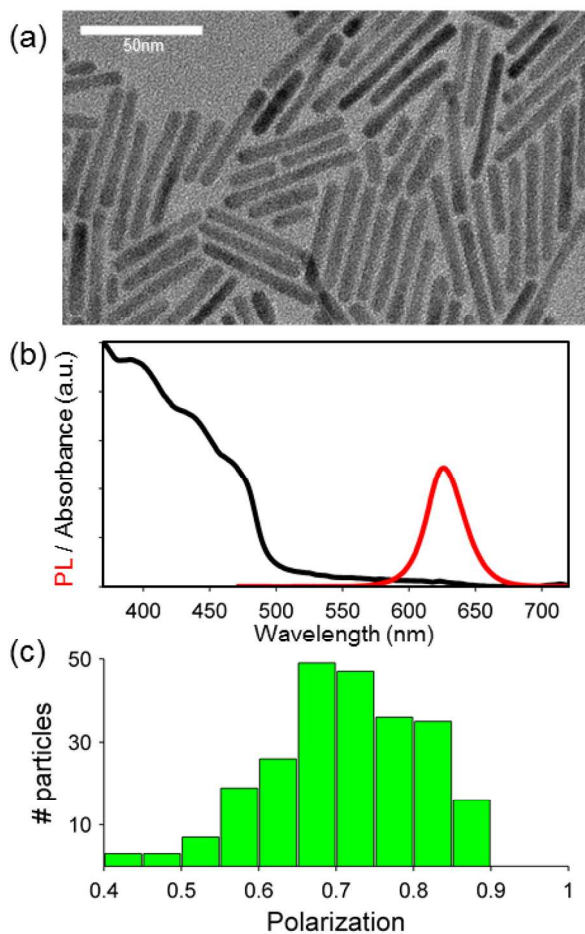


Figure S3. Seeded NR sample with wider size distribution (average dimensions 49 nm x 5 nm). (a) TEM image of the studied nanorods shows differences in sizes – length in particular, between the rods. (b) Absorption and PL spectra of the sample. The features in the absorption spectrum are broadened, indicating a wide distribution in the electronic transitions energies. (c) Histogram of polarization values obtained from 240 single S@R particles yielding average polarization of 0.74 and STD of 0.09.

4. Calculating single particle polarization out of PS anisotropy

The procedure for calculating the anisotropy coefficient for a sample of nanorods in solution with random orientation and known absorption and emission factors is described in our previous article¹ and a detailed theory can be found in text books^{2,3}. Briefly, if the rod is described as a cylinder and the polarization factor for absorption (emission) is set as the ratio of absorption (emission) between the cylinder ‘out-of-plane’ axis and ‘in-plane’ axes, one can integrate the probability for absorbance and emission of a photon over all possible orientations and obtain the anisotropy factor. By repeating this procedure for various values of absorption and emission factors, an anisotropy map is constructed, and can be used for calculating polarization factors from known anisotropy value (Figure S4). In this case we measured the emission polarization factor directly by single particle polarization measurement, and we also measured the ensemble anisotropy for the same samples. Using the above method we were able to calculate the band-edge absorption degree of polarization.

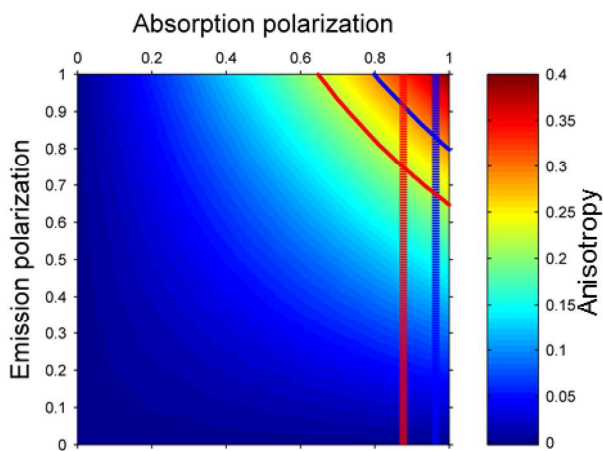


Figure S4. Photoselection anisotropy map as a function of the absorption and emission polarization factors (reprinted from ref 1). Blue (Red) isoline represents the R@R (S@R) measured anisotropy coefficient ($r_{R@R}=0.29$ $r_{S@R}=0.22$). Vertical dashed lines indicate the absorption polarization values (absorption polarization $p_{R@R}=0.97$, $p_{S@R}=0.88$) for measured emission polarization factors (emission polarization – $p_{R@R}=0.83$ & $p_{S@R}=0.75$).

- (1) Sitt, A.; Salant, A.; Menagen, G.; Banin, U. Highly Emissive Nano Rod-in-rod Heterostructures with Strong Linear Polarization. *Nano Lett.* **2011**, *11*, 2054–2060.
- (2) Kliger, D. S.; Lewis, J. W.; Einterz, R. C. *Polarized Light in Optics and Spectroscopy*; 1st ed.; Academic Press Inc.: San Diego, 1990.
- (3) Lakowicz, J. R. *Principles of Fluorescence Spectroscopy*; 3rd ed.; Springer: Singapore, 2006.